Original Article

Cytogenet Genome Res 107:68–76 (2004)
DOI: 10.1159/000079573

Cytogenetic and Genome Research

Cloning of the breakpoints of a de novo inversion of chromosome 8, inv (8)(p11.2q23.1) in a patient with Ambras syndrome

M. Tadin-Strapps,[a] D. Warburton,[b,c] F.A.M. Baumeister,[e] S.G. Fischer,[d] J. Yonan,[d] T.C. Gilliam[c,d] and A.M. Christiano[a,c]

Departments of [a] Dermatology, [b] Pediatrics and [c] Genetics and Development, [d] Columbia Genome Center, Columbia University, New York, NY (USA); [e] Children's Hospital of the Technical University, Munich (Germany)

Abstract. Ambras syndrome (AMS) is a unique form of universal congenital hypertrichosis. In patients with this syndrome, the whole body is covered with fine long hair, except for areas where normally no hair grows. There is accompanying facial dysmorphism and teeth abnormalities, including retarded first and second dentition and absence of teeth. In 1993, Baumeister et al. reported an isolated case of Ambras syndrome in association with a pericentric inversion of chromosome 8. Subsequently, another patient with congenital hypertrichosis and rearrangement of chromosome 8 was reported by Balducci et al. (1998). Both of these patients have a breakpoint in 8q22 in common suggesting that this region of chromosome 8 contains a gene involved in regulation of hair growth. In order to precisely determine the nature of the rearrangement in the case of Ambras syndrome, we have used fluorescent in situ hybridization (FISH) analysis. We have cloned the inversion breakpoints in this patient and generated a detailed physical map of the inversion breakpoint interval. Analysis of the transcripts that map in the vicinity of the breakpoints revealed that the inversion does not disrupt a gene, and suggests that the phenotype is caused by a position effect.

Ambras syndrome (AMS) is a unique form of universal congenital hypertrichosis (MIM 145701) that has been described in only eleven cases in the medical literature so far (Baumeister et al., 1993; Balducci et al., 1998; Torbus and Sliwa, 2002). This syndrome is characterized by excessive hair growth over the entire body except for the areas in which no hair normally grows (palms, soles, mucosae). Hypertrichosis is accentuated on the shoulders, the face, and the ears (Baumeister et al., 1993). Minor facial and dental anomalies, such as retarded first and second dentition and absence of teeth have also been reported. Familial cases suggest a genetic basis for this form of hypertrichosis (Nowakowski and Schloz, 1977; Baumeister et al., 1993), but the gene(s) involved remain unknown.

The Ambras case reported by Baumeister et al. (1993), patient ME-1, was reported in association with a de novo pericentric inversion of chromosome 8, inv (8)(p11.2q22). Interestingly, in 1998 another patient with congenital hypertrichosis and rearrangement of chromosome 8 was reported by Balducci et al. in association with a de novo paracentric inversion of chromosome 8, inv (8)(q12q22). Both of these patients have a breakpoint in 8q22 in common suggesting that this region of chromosome 8 contains a gene involved in regulation of hair growth.

In a search for a gene whose mutations lead to hypertrichosis, we have performed cytogenetic and molecular analysis in both of these two patients. Our analysis of patient SS-1, originally reported by Balducci et al. (1998), was published previously (Tadin et al., 2001).

In this work, we report detailed cytogenetic and molecular analysis in patient ME-1, originally reported by Baumeister et al. (1993), and cloning of the inversion breakpoints. Our findings are in agreement with the initial cytogenetic diagnosis of an apparently balanced pericentric inversion of chromosome 8. We were also able to refine the inversion breakpoints to 8p11.2 and 8q23.1, inv (8)(p11.2q23.1). In order to characterize the

This work was supported in part by the Skin Disease Research Center in the Department of Dermatology at Columbia University (USPHS P30-44345) and the Dermatology Foundation.

Received 27 April 2004; manuscript accepted 5 May 2004.

Request reprints from: Dr. Angela M. Christiano, Department of Dermatology
Columbia University College of Physicians and Surgeons
630W 168th Street, VC15-216, New York, NY 10032 (USA)
telephone: +1-212-305-9565; fax: +1-212-305-7391
e-mail: amc65@columbia.edu

inversion breakpoint region more precisely, we have generated a detailed physical map of the 8q22→q24 region and mapped all transcripts in the vicinity of the 8q23 breakpoint. We found that the inversion of chromosome 8 in this patient does not cause disruption of a gene from this interval, suggesting that the phenotype most likely results from a position effect caused by this cytogenetic rearrangement.

Materials and methods

Patient materials

Patient ME-1 was originally reported by Baumeister et al. (1993). The girl was the product of a normal pregnancy and had no family history of hypertrichosis. As a newborn, she was completely covered with fine long hair that was lightly pigmented and 1–2 cm in length. In addition to hypertrichosis, the patient had bilateral accessory nipples and ulnar rudimentary hexadactyly. No other abnormalities were detected upon ultrasound of the abdomen and determination of plasma androgen levels. Cytogenetic analysis revealed an apparently balanced pericentric inversion of chromosome 8 with breakpoints in p11.2 and q22, inv (8)(p11.2q22) (Baumeister et al., 1993).

Transformed lymphoblast cell lines were generated for the patient and her unaffected parents by EBV transformation using standard procedures (Speck and Strominger, 1987). Genomic DNA was isolated from lymphoblastoid cell lines using the Blood and Cell Culture DNA Maxi Kit (Qiagen).

Contig assembly

YAC clones were selected from the Whitehead Institute STS-based map on the basis of STS markers that were mapped to 8q22, 8q23, and 8q24, and obtained from Research Genetics. DNA was isolated as described by Hoffman and Winston (1987), and tested for STS content by the polymerase chain reaction (PCR) according to Research Genetics' Genome Services Protocol (http://www.researchgenetics.com). Sequences for the STS markers are available from the Genome Database (http://www.gdb.org).

BAC clones from the interval were selected from the NCBI database on the basis of the available sequence data and obtained from Research Genetics and from Keio University Genomics Research Institute. Clone overlaps were detected by using BLAST, available at the National Center for Biotechology Information, (http://www.ncbi.nlm.nih.gov/BLAST) and were verified by PCR.

BAC DNA was isolated using Large-Construct Kit (Qiagen) according to the manufacturer's instructions. For STS content PCR, 100 ng of BAC DNA was amplified using Platinum Taq PCR Supermix (Invitrogen) in a cocktail containing 10 pmol of forward and reverse primer in a total volume of 30 µl. PCR amplification of BAC DNA was performed under the following conditions: 95 °C for 5 min, followed by 35 cycles of denaturation (94 °C for 30 s), annealing (55 °C for 30 s), and elongation (72 °C for 30 s), and a final elongation step at 72 °C for 7 min. PCR products were resolved on 1 % agarose gels and visualized by ethidium bromide staining. In addition to the available STS markers, additional PCR primers were generated for use in clone overlap verification: 680F23 3′ F: 5′-ATG GGT GGG CCT GAG TAT TT-3′ R: 5′-AGG TAA AGC TGC CCA AAC CT-3′; 659A24 5′ F: 5′-AAC CCT GAG AGG CAC TCT GT-3′ R: 5′-ATG GGG TCC CTG TTC TCT CT-3′.

FISH analysis

YAC and BAC DNA was DIG-labeled with a DIG-Nick Translation Mix kit (Roche Molecular Biochemicals) according to the manufacturer's instructions. Labeled probe was precipitated with Cot-1 DNA (10 µg of Cot-1 DNA per 100 ng labeled probe) and resuspended in Hybrisol VII (ONCOR) to a final concentration of 2 ng/µl.

Metaphase chromosome spreads were prepared from the transformed lymphoblast cell lines by standard laboratory procedures. FISH analysis was performed as previously described (Tadin et al., 2001). Definite chromosomal assignment was verified by co-hybridization with chromosome 8 centromere-specific probe (D8Z2) (ONCOR). Chromosomes were counterstained with DAPI (VYSIS) and viewed using a Nikon microscope fitted with a filter wheel and Cytovision Applied Imaging software.

Southern analysis and restriction mapping

Genomic DNA (10 µg) was digested in a total volume of 60 µl at 37 °C overnight as either a single or double digest with *Eco*RV, *Pst*I, *Nhe*I, *Xho*I, and *Hin*dIII according to the manufacturer's instructions (NEBiolabs). Restriction products were run on a 0.7 % agarose gel at 55 V for 16 h.

Probes used in Southern blot analysis were PCR amplified from human normal control genomic DNA using primers specific to the BAC clone KB1153C10 (Acc# AP001331). The probe MT6, that detects the rearranged allele in the patient sample, recognizes a 490-bp fragment of the clone KB1153C10 (40,807–41,297 bp on sequence Acc# AP001331). PCR primers used to amplify this fragment are MT6F 5′-GGA GTA CCA CGA GCA ATA CAG-3′ and MT6R 5′-AAC TCG GTG AGT ACA GCT AGC-3′. Probes were labelled with [α-^{32}P]dCTP in a random priming reaction using Prime-It II Random Primer Labelling Kit (Stratagene). Southern blot analysis was performed using standard protocols.

Computational sequence analysis

Sequence analysis of the BAC clone KB1152C10 was performed using BLAST tool against the *nt* and the *dbEST* databases at the NCBI (http://www.ncbi.nlm.nih.gov), and using the Human Genome Browser at UC Santa Cruz (http://genome.ucsc.edu).

Breakpoint subcloning

The breakpoint was subcloned using the inverse polymerase chain reaction (IPCR) technique (Wagner et al., 2002), see Fig. 4. Briefly, genomic DNA from the patient and a control individual was digested with *Pst*I in a total volume of 20 µl at 37 °C overnight. 20 µl of each digest were then self-ligated with 5 µl of T4 DNA ligase (NEBiolabs) in a total reaction volume of 100 µl. Ligation reactions were heat-inactivated at 70 °C for 5 min.

1 µl of the ligation reactions was used as a template in a nested PCR reaction with the following primers: Primer pair 1 forward (primer D): 5′-TCC TGC TGG AAA CTC CTA GTG C-3′, Primer pair 1 reverse (primer C): 5′-GGC AGG CTC TAA CTG ACA CTC A-3′; Primer pair 2 forward (primer B): 5′-TCT TCC AGA GCA TAA CCA TTG C-3′, Primer pair 2 reverse (primer A): 5′-GAT TCA GGA TGC AGT GAG AAG C -3′. PCR was performed with Advantage-2 Kit (Clontech). PCR products were gel-purified using the Rapid Gel Purification Kit (Invitrogen), subcloned, and sequenced on an ABI Prism 310 sequencer (P.E. Biosystems).

Once one of the 8p/8q breakpoint junctions was sequenced, additional PCR primers were designed on the basis of known sequence to test for possible deletions and/or duplications that might have resulted from the inversion event. PCR primers 8p′′′ 5′-AAG TCA AAA TCA CTC CTT GGG C-3′ and 8q′′′ 5′-gac ata ggc atg ggc aaa gac t-3′ were used for "breakpoint-specific" PCR. A 1.8-kb PCR product, containing the other inversion breakpoint fusion, was obtained only for the patient but not for the control individuals. This band was gel purified and sequenced as described above.

Results

In order to physically narrow the region containing the inversion breakpoint in the long arm of chromosome 8, we used FISH analysis with large YAC and BAC clones that have been mapped to 8q23. Since no comprehensive integrated map of chromosome 8 was available at the outset of this study, we assembled a contig of YAC and BAC clones across the inversion breakpoint interval on the basis of STS content. First, a "backbone" of YAC clones was assembled using STS markers that were mapped to 8q22→q24. The interval was then further saturated with BAC clones that have been mapped to this region on the basis of the available sequence data. Both computer sequence analysis and PCR confirmed overlaps between BAC clones.

The detailed physical map of the 8q22→q24 region is shown in Fig. 1. YAC clones are indicated in the top half of the figure and are oriented relative to one another on the basis of

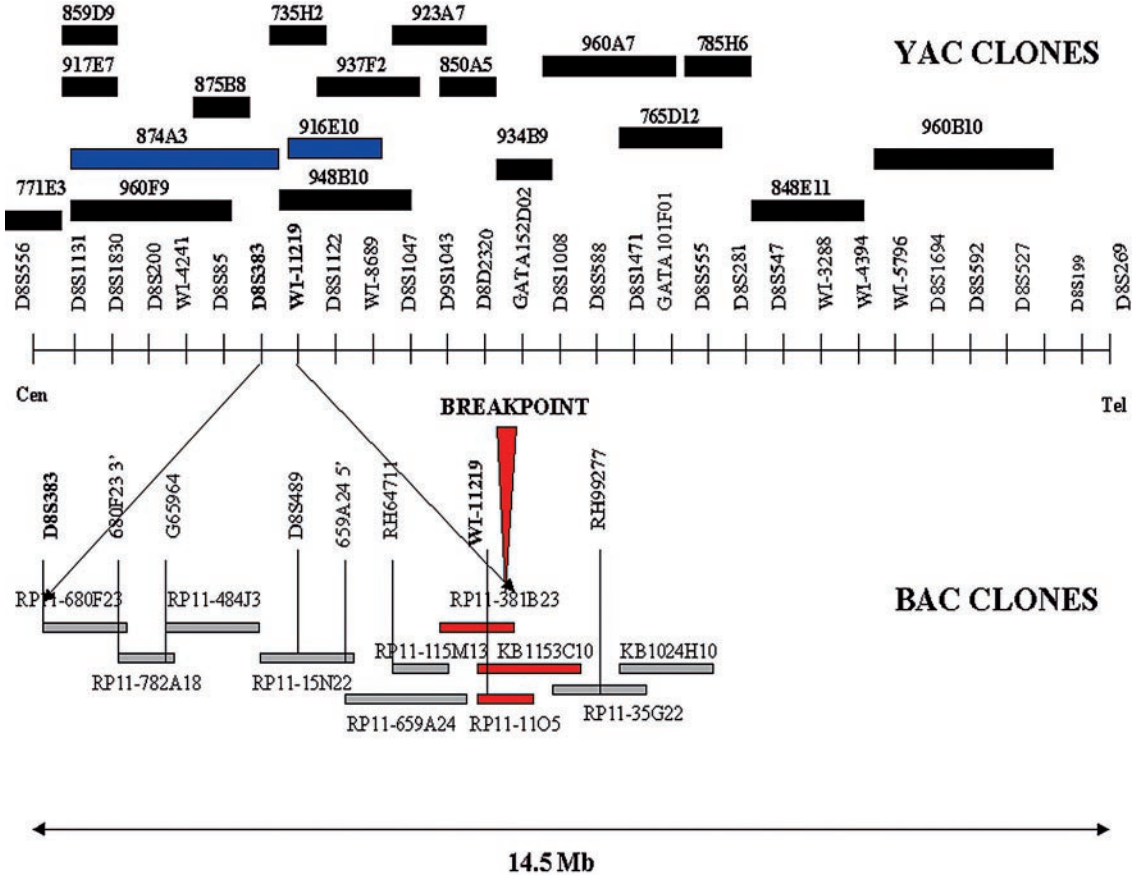

Fig. 1. A detailed 14.5-Mb physical map of the 8q23 inversion breakpoint in patient ME-1. YAC and BAC clones are ordered into a contig on the basis of STS content. The positions of the STS markers on YAC and BAC clones are indicated by thin vertical lines. Initial FISH analysis mapped the breakpoint between YAC clones 874A3 (proximal to the breakpoint) and 916E10 (distal to the breakpoint) shown in blue. The interval between these two clones, defined by STS markers D8S383 and WI-11219 (bold), was then saturated with additional BAC clones in order to narrow the breakpoint interval even further. The position of the inversion breakpoint is shown with a red triangle. BAC clones indicated in red RP11-381B23, RP11-11O5, and KB1153C10 encompass the breakpoint in patient ME-1.

Fig. 2. A schematic representation of YAC and BAC FISH probes used in analysis on metaphase chromosomes obtained from patient ME-1. FISH probes are indicated as differently colored bars that are positioned relative to the chromosome as they hybridized to the normal 8 (left) and the rearranged 8 (right). YAC clones indicated in red were found to be distal, and those indicated in blue proximal to the breakpoint. Like YACs, BAC clones that hybridized distal to the break are shown as smaller red bars and those that hybridized proximal to the break as smaller light blue bars. Clones shown in light green generated signals on both arms of the rearranged chromosome indicating that they encompass the breakpoint.

Fig. 3. (**A**) An example of FISH analysis with BAC clone KB1153C10. Hybridization of the BAC clone is indicated as a red signal. The green signal corresponds to chromosome 8 centromere-specific probe (D8Z2). On the normal chromosome 8 there is only one red signal on the q arm (arrow head). On the rearranged 8, the BAC clone hybridizes to both chromosome arms indicating that it encompasses the breakpoint (arrows). (**B**) Southern blot analysis with genomic DNA from the lymphoblast cell line from the patient (P) and a control (N). M denotes molecular size marker. DNA was digested with *Nhe*I and *Pst*I as a single digest or with *Pst*I/*Nhe*I, *Xho*I/*Eco*RV, and *Hin*dIII/*Eco*RV as a double digest. The probe used in this Southern analysis was MT6. The relative positions of the restriction sites, the MT6 probe, and the breakpoint are shown in the bottom right. (**C**) Location of genes and EST clones on the clone KB1153C10. Exons of eukaryotic translation initiation factor 3, subunit 6, EIF3S6 gene (also known as INT6) are shown as green bars. The 5′ end of the I.M.A.G.E. clone 5201681, encoding a novel thrombospondin-like gene (THBSL1) overlaps with the first 11 kb of the BAC clone KB1153C10, whereas the 3′ end extends to another BAC clone located more proximally. The CpG island located just slightly upstream of the start codon of THBSL1 is indicated as a blue diamond. The location of the breakpoint on BAC KB1153C10 is indicated by a red arrow.

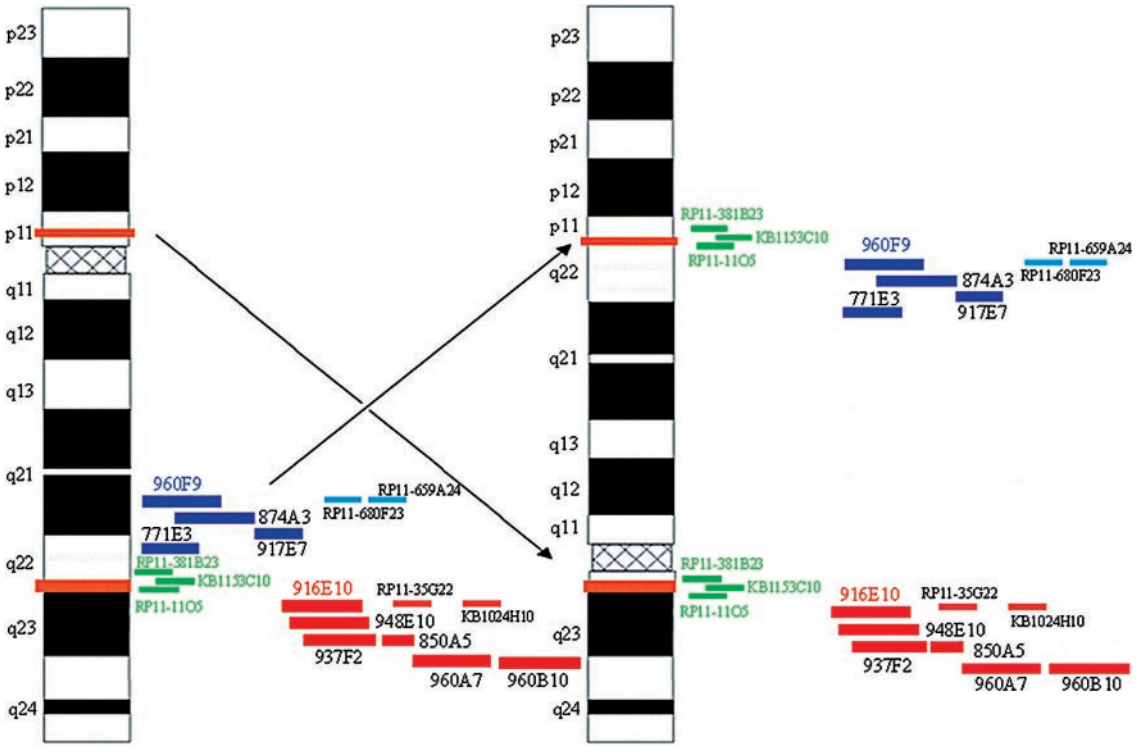
p23
p22
p21
p12
p11
q11
q12
q13
q21
q22
q23
q24
960F9
874A3
771E3
917E7
RP11-659A24
RP11-680F23
RP11-381B23
KB1153C10
RP11-11O5
916E10
RP11-35G22
948E10
KB1024H10
850A5
937F2
960A7
960B10

2

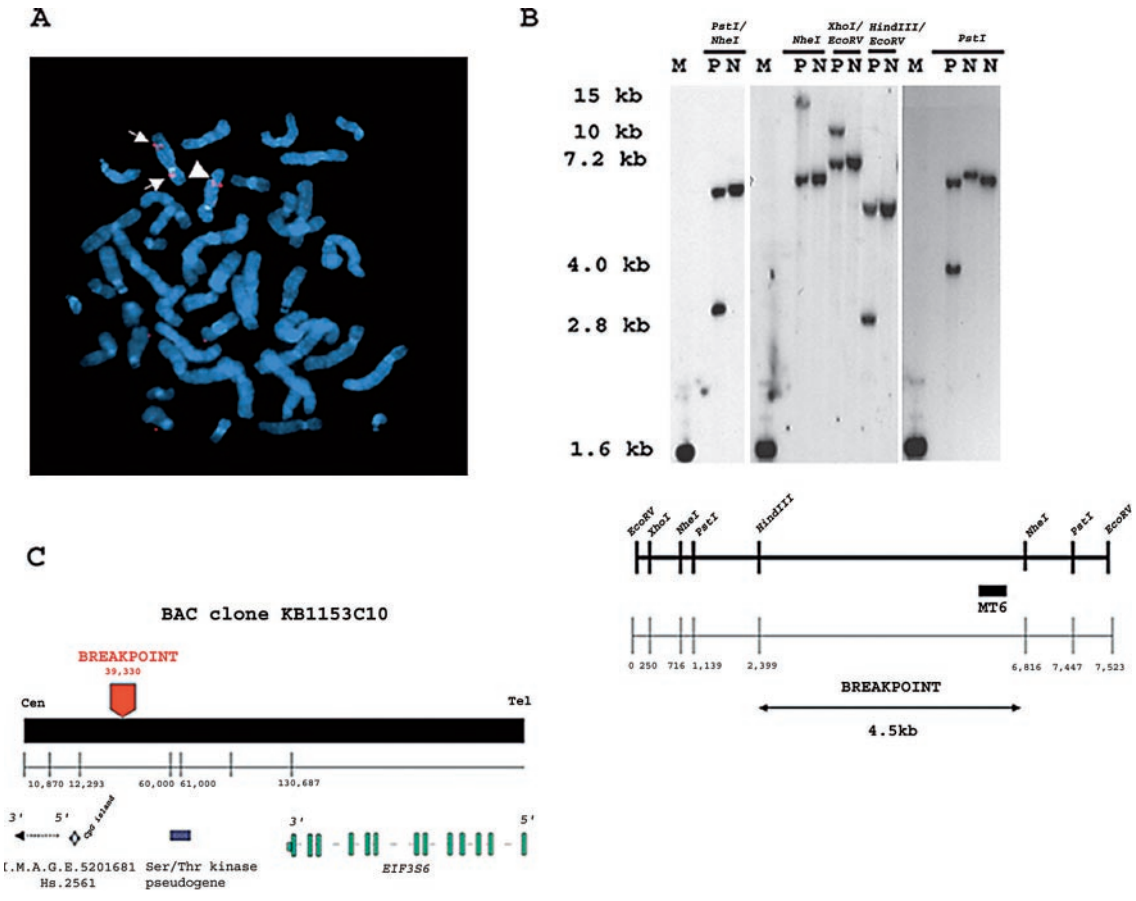
A
B
C
M
P
N
15 kb
10 kb
7.2 kb
4.0 kb
2.8 kb
1.6 kb
PstI/ NheI
XhoI/ EcoRV
HindIII/ EcoRV
PstI
EcoRV
XhoI
NheI
PstI
HindIII
MT6
BREAKPOINT
4.5kb
BAC clone KB1153C10
Cen
Tel
39,330
10,870
12,293
60,000
61,000
130,687
CpG island
Ser/Thr kinase pseudogene
Hs.2561
EIF3S6

3

STS markers. Initial FISH analysis mapped the breakpoint between YAC clones 874A3 (proximal to the breakpoint) and 916E10 (distal to the breakpoint). The interval between these two YAC clones (between STS markers D8S383 and WI-11219) was then saturated with additional BAC clones in order to narrow the inversion breakpoint interval even further. The bottom half of Fig. 1 depicts an expanded view of the interval between markers D8S383 and WI-11219 with all the BAC clones that were mapped to this region. FISH analysis with these clones revealed that clones RP11-381B23, RP11-11O5, and KB1153C10 (shown in red in Fig. 1) encompass the breakpoint since all three generated split hybridization signals on both arms of the rearranged chromosome 8 (Fig. 3A).

Results from our FISH analysis are summarized in Fig. 2. We used over twenty FISH probes to characterize the cytogenetic rearrangement in this patient and to precisely map the 8q inversion breakpoint. Comparison of the hybridization signals obtained from the normal and the rearranged chromosomes 8 enabled us to determine which clones were proximal and which distal to the breakpoint, and to narrow the inversion breakpoint interval. We identified three BAC clones that span the 8q breakpoint, RP11-381B23, RP11-11O5, and KB1153C10 (Fig. 2). This observation mapped the breakpoint to the region of overlap between the three BAC clones corresponding to a genomic interval of about 100 kb. Our cytogenetic findings are in agreement with the original report of patient ME-1 (Baumeister et al., 1993), in that this patient has an apparently balanced pericentric inversion of chromosome 8. Using the newly available information on the physical location of BAC clones from this interval (available at the UC Santa Cruz website), we were also able to refine the 8q breakpoint to the band 8q23.1, slightly more distal than is revealed by G-banding alone.

We took advantage of the fact that the entire sequence of the split clone KB1153C10 (Acc# AP001331) was known, and utilized this to design probes for Southern analysis. In order to map the breakpoint region on the BAC KB1153C10, we chose restriction enzymes with recognition sites approximately every 5–10 kb throughout the BAC clone. We then designed PCR primers that amplify 500–600 bp segments within each restriction fragment to be used as probes in Southern analysis (Fig. 3B). In this way, we mapped the breakpoint to an *Eco*RV fragment between 34,481 bp and 42,004 bp on clone KB1153C10. Using additional restriction enzymes, we were able to generate a detailed restriction map of the breakpoint interval and narrow this region to about 4-kb (Fig. 3B).

Figure 3C illustrates the location of genes, ESTs and putative transcripts within clone KB1153C10 with respect to the breakpoint. The only known gene on this clone is eukaryotic translation initiation factor 3, subunit 6, EIF3S6 (also known as INT6). The 3′ end of INT6 is located about 90 kb distal to the breakpoint (Fig. 3C). The other two transcripts that map to BAC KB1153C10 are a Ser/Thr aurora-like kinase gene prediction and a novel gene with similarity to thrombospondin that we named thrombospondin-like 1, THBSL1 (Fig. 3C). The 5′ end of the THBSL1 transcript, (I.M.A.G.E. EST clone 5201681) overlaps with the first 11 kb of clone KB1153C10. The 3′ end of this gene overlaps with an adjacent BAC clone, RP11-659A24 (Acc# AC025508), that is proximal to the breakpoint (Fig. 1 and 2). Finally, we also identified a CpG island in this region that maps just upstream of the putative start site of transcript of THBSL1 (Fig. 3C). Genomic sequence analysis of the Ser/Thr aurora-like kinase prediction revealed that this is most likely a pseudogene since the putative mRNA moves in and out of the translational reading frame. We were also unable to detect expression of this transcript from a panel of different cDNAs by RT-PCR analysis (data not shown).

In order to clone and characterize the 8p/8q inversion breakpoints, we used the inverse polymerase chain reaction (IPCR) and our knowledge of the 8q23 breakpoint restriction map. For the purpose of clarity, we designated the two inversion breakpoint junctions 1 and 2 (Fig. 4 and 5). Our strategy for cloning the 8p/8q breakpoint junction 1 is illustrated in Fig. 4A. Based on Southern analysis with MT6 probe (Materials and methods), we knew that *Pst*I generates a 6-kb band from the wild-type allele and a 4-kb band from the rearranged chromosome 8 (Fig. 3B). Using IPCR, we were able to obtain an approximately 4-kb PCR product from the inverted chromosome containing the unknown sequence from 8p that is centromeric to the breakpoint 1, the *Pst*I site used for digestion and ligation, and the sequence within the 8q that is telomeric to the breakpoint (Fig. 4). The expected IPCR product was only observed from the DNA of the patient, but not when the same experiment was performed using genomic DNA from a control individual (data not shown). Sequence analysis of the IPCR product with the BLAST tool identified a perfect match

Fig. 4. Cloning of the 8p/8q inversion breakpoint junction 1. (**A**) Schematic representation of the normal and the inverted chromosomes 8 and the location of the *Pst*I recognition sites in the vicinity of the inversion breakpoints (red triangles). Following inversion, the position of the *Pst*I sites relative to the breakpoints changes. This change can be detected in Southern analysis since the *Pst*I fragment obtained from the wild type allele differs in size from that obtained from the inverted chromosome, 6 kb versus 4 kb. For the inverse polymerase chain reaction (IPCR), genomic DNA from patient ME 1 was digested with *Pst* I, self-ligated, and used as a template in a PCR reaction with either primers C and D or with primers A and B. PCR primers were generated on the basis of known sequence from 8q23. (**B**) Sequence across the inversion breakpoint junction 1. The alignments show from top to bottom: the 8p11.2 sequence centromeric to the breakpoint that is homologous to BAC clone AC092818, 8p/8q breakpoint junction 1, and the 8q23.1 sequence telomeric to the breakpoint that is homologous to BAC clone AP001331. The boxes indicate the homologies between the three sequences. Note a 5-bp insertion at the breakpoint junction. The orientation of the BAC clones on the chromosome is indicated.

Fig. 5. Cloning of the 8p/8q inversion breakpoint junction 2. (**A**) Once the sequence of one end of the 8p/8q inversion was known, additional PCR primers were designed to specifically amplify the other end of the inversion. Primers 8p‴ and 8q‴ (shown in purple) specifically amplify the breakpoint junction 2 from the rearranged allele. The location of the primers is shown on both the wild type and the inverted chromosomes. Primers used for IPCR (A, B, C, and D) are also shown for comparison. (**B**) Sequence around the breakpoint junction 2. The alignments shown from top to bottom: the 8p11.2 sequence telomeric to the breakpoint that is homologous to BAC clone AC092818, the 8p/8q breakpoint junction 2, and the 8q23.1 sequence centromeric to the breakpoint that is homologous to BAC clone AP001331. Note a 2-bp insertion at the breakpoint junction. The orientation of the BAC clones on the chromosome is indicated. (**C**) Results of the "breakpoint-specific" PCR. The 1.8-kb fragment is obtained only from the patient's genomic DNA but not from the two control individuals.

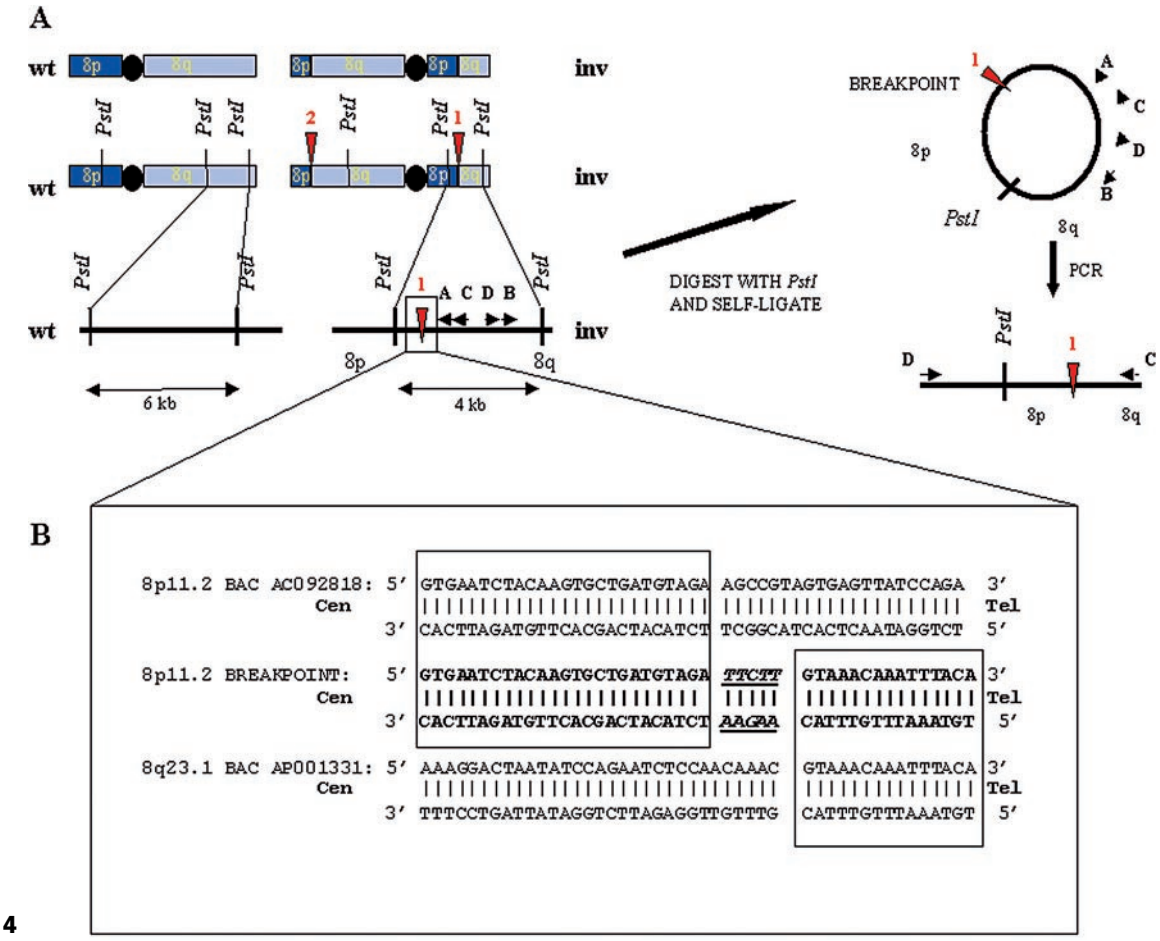
A
wt
inv
PstI
8p
8q
6 kb
4 kb
DIGEST WITH PstI
AND SELF-LIGATE
BREAKPOINT
PCR
B
8p11.2 BAC AC092818: 5′ GTGAATCTACAAGTGCTGATGTAGA AGCCGTAGTGAGTTATCCAGA 3′
Cen Tel
3′ CACTTAGATGTTCACGACTACATCT TCGGCATCACTCAATAGGTCT 5′
8p11.2 BREAKPOINT: 5′ GTGAATCTACAAGTGCTGATGTAGA TTCTT GTAAACAAATTTACA 3′
Cen Tel
3′ CACTTAGATGTTCACGACTACATCT AAGAA CATTTGTTTAAATGT 5′
8q23.1 BAC AP001331: 5′ AAAGGACTAATATCCAGAATCTCCAACAAAC GTAAACAAATTTACA 3′
Cen Tel
3′ TTTCCTGATTATAGGTCTTAGAGGTTGTTTG CATTTGTTTAAATGT 5′

4

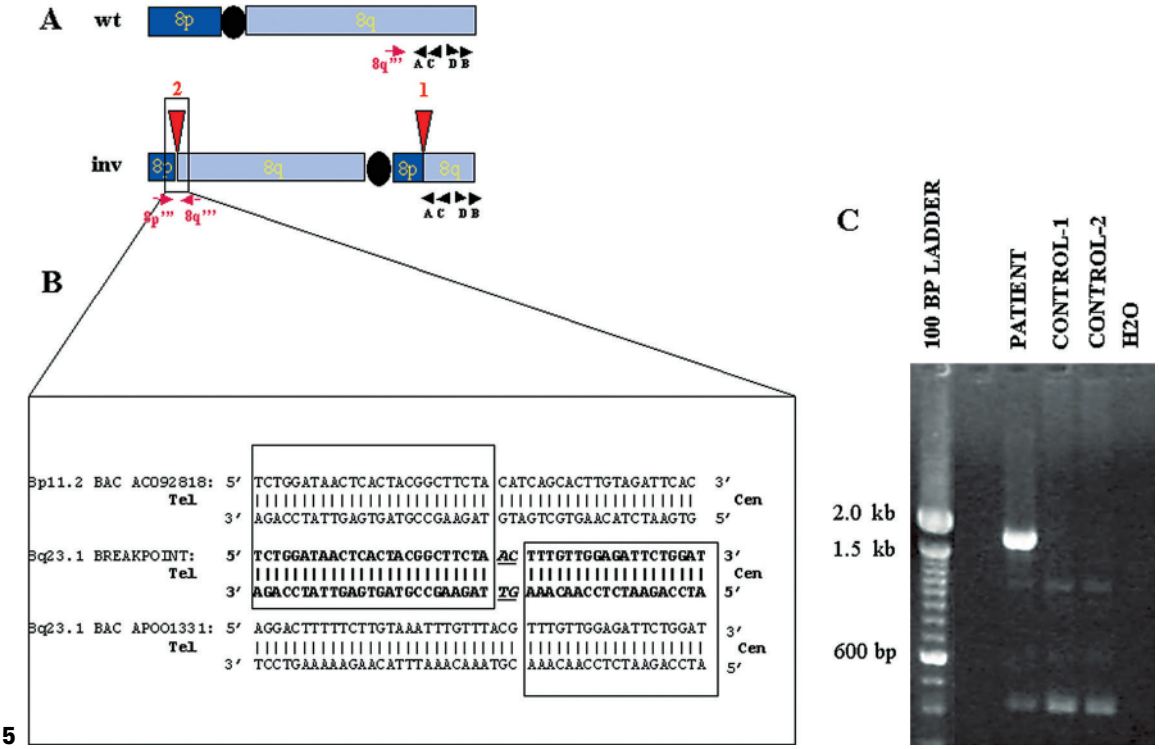
A
wt
inv
8q‴
AC DB
B
8p‴ 8q‴
8p11.2 BAC AC092818: 5′ TCTGGATAACTCACTACGGCTTCTA CATCAGCACTTGTAGATTCAC 3′
Tel Cen
3′ AGACCTATTGAGTGATGCCGAAGAT GTAGTCGTGAACATCTAAGTG 5′
8q23.1 BREAKPOINT: 5′ TCTGGATAACTCACTACGGCTTCTA AC TTTGTTGGAGATTCTGGAT 3′
Tel Cen
3′ AGACCTATTGAGTGATGCCGAAGAT TG AAACAACCTCTAAGACCTA 5′
8q23.1 BAC AP001331: 5′ AGGACTTTTTCTTGTAAATTTGTTTACG TTTGTTGGAGATTCTGGAT 3′
Tel Cen
3′ TCCTGAAAAAGAACATTTAAACAAATGC AAACAACCTCTAAGACCTA 5′
C
100 BP LADDER
PATIENT
CONTROL-1
CONTROL-2
H2O
2.0 kb
1.5 kb
600 bp

5

between the unknown sequence from 8p and a segment of the BAC clone RP11-419C23 (Acc# AC092818) that maps to 8p11.2.

In order to clone and characterize the other inversion breakpoint junction (junction 2), and to determine whether the inversion event resulted in insertions/deletions within either 8p11.2 or 8q23.1, we designed additional PCR primers within 8q23.1 and 8p11.2 (Fig. 5A). Using PCR primers 8q‴ and 8p‴, we were able to obtain a 1.8-kb PCR product that contains the sequence from 8p that is telomeric to the breakpoint junction 2, the 8q/8p breakpoint junction, and the sequence from 8q23.1 that is centromeric to the breakpoint (Fig. 5B). This "breakpoint-specific" PCR resulted in a 1.8-kb product only when DNA from the patient ME-1 was used as a template, but not when DNA from control individuals was used (Fig. 5C).

Sequence analysis of the 8p/8q breakpoint junctions revealed a 5-bp "TTCTT" insertion at the breakpoint junction 1 (Fig. 4B) and a 2-bp "AC" insertion at the breakpoint junction 2 (Fig. 5B). Reconstitution of the sequences of the 8p and 8q breakpoint junctions revealed that the inversion event also resulted in a deletion of a "C" nucleotide from the q arm just before the "TTCTT" insertion, and a "TAGA" duplication on the p arm on both sides of the "AC" insertion (data not shown). Analysis of the genomic sequence surrounding the inversion breakpoints revealed that the inversion event did not disrupt the coding or nearby regulatory sequence of a gene, but rather that both breakpoints occur within repetitive DNA. On the p arm, the break disrupts a Tigger 1 repetitive element, whereas on the q arm, the break occurs within a LINE-1 element. We were unable to detect any sequence homology in regions surrounding the inversion breakpoints.

Based on the observation of another case of congenital hypertrichosis and rearrangement of 8q, we focused our molecular analysis on this arm of chromosome 8. However, we wanted to exclude the possibility that inversion in patient ME-1 actually disrupts a gene on the p arm. Genomic sequence analysis of the region on the BAC clone RP11-419C23 surrounding the 8p breakpoint junction revealed the absence of any known genes in the vicinity of the breakpoint (data not shown). FKSG2, an apoptosis inhibitor, is the only known gene in this interval and maps to 8p12 almost 200 kb 5′ (telomeric) to the breakpoint. In the interval 3′ (centromeric) to the 8p breakpoint the first transcript, FLJ14299, maps almost 600 kb away from the breakpoint. FLJ14299 is a novel gene of unknown function.

Discussion

Cytogenetic mapping is a powerful tool for identification of disease genes. There are many examples of human diseases in which analysis of chromosomal anomalies have subsequently led to discovery of disease critical intervals, and eventually lead to identification of genes involved in the etiology of a disease. Among these are holoprosencephaly (Belloni et al., 1996), hand-and-foot syndrome (Crackower et al., 1996), aniridia (Gessler et al., 1989), and X-linked ectodermal dysplasia (Srivastava et al., 1996), among others.

In our effort to clone the Ambras hypertrichosis gene, we have performed extensive cytogenetic and molecular analysis in a patient with AMS carrying a pericentric inversion of chromosome 8, inv (8)(p11.2q23.1). Since congenital universal hypertrichosis is a very rare condition, and rearrangement of 8q23 was reported in another patient with congenital hair overgrowth (Balducci et al., 1998; Tadin et al., 2001), we focused our analysis on the inversion breakpoint within the q arm of the chromosome. We have assembled a detailed physical map of the 8q22→q24 breakpoint interval and mapped all transcripts in the vicinity of this breakpoint. Cloning of the breakpoints revealed that the inversion does not disrupt a gene, but rather occurs in a non-coding DNA. On the q arm, the break occurs between the INT6 gene, which is distal to the breakpoint and maps about 90 kb upstream, and a novel thrombospondin-like gene, THBSL1, which maps about 30 kb proximal to the breakpoint. We also analyzed genomic sequences surrounding the 8p breakpoint to exclude the possibility that the observed phenotype is due to a disruption of a gene on this arm of the chromosome. Here too the inversion breakpoint occurs within extragenic DNA and the nearest transcripts in the vicinity of the breakpoint map 200 kb telomeric and almost 600 kb centromeric to the break.

Several lines of evidence suggest that INT6 acts to prevent breast tumorigenesis in humans and mice (Rasmussen et al., 2001; Marchetti et al., 1995). INT6 is expressed ubiquitously and early in embryogenesis in mice. Studies in yeast suggest that INT6 may function in chromosome stability (Yen at al., 2003). Amino acid sequence analysis revealed similarity to eukaryotic translation initiation factors, but the exact function of this gene remains largely unknown. Considering the ubiquitous expression of INT6 and its potential role in translation regulation and chromosome stability, we consider INT6 an unlikely candidate for Ambras syndrome.

Another transcript identified in the vicinity of the breakpoint in patient ME-1 is a novel thrombospondin-like gene, THBSL1. Thrombospondins are a family of extracellular modular glycoproteins (Adams and Tucker, 2000). Interestingly, thrombospondin 1 (THBS1) has been implicated in the control of hair follicle involution (Yano et al., 2003). However, the effects of THBS1 on the hair growth and cycling seem to be associated with changes in perifollicular vascularization and vascular proliferation, which, to our knowledge, are not observed in Ambras patients. The 5′ end of the THBSL1 gene was mapped about 30 kb centromeric to the breakpoint in patient ME-1. Genomic sequence analysis in this interval revealed the presence of a CpG island that maps just upstream of the putative start site of the transcript. However, it remains to be determined whether the region upstream of the cDNA start site contains enhancer elements that may have been disrupted in the inversion event.

Little is known about the mechanism of de novo balanced rearrangements. These are very rare events and are thought to occur randomly. Our finding that one of the breakpoints occurs within a Tigger-1 DNA transposon is noteworthy since a transposon-mediated recombination has been proposed as the mechanism for generating rearrangements in patients with Charot-Marie-Tooth disease type 1A (CMT1A) and hereditary

neuropathy with liability to pressure palsies (HNPP) (Reiter et al., 1996). Tigger-1 is a DNA transposon-like element that closely resembles the *Drosophila pogo* DNA transposon (Smith and Riggs, 1996). Among all DNA transposon-like elements that make up about 1% of the human genome, there are about 3,000 Tigger-1 elements (Smith and Riggs, 1996). Tigger elements are thought to have originated about 80–90 millions of years ago in an early primate or primate ancestor (Robertson, 1996). In *Drosophila*, transposable elements have been shown to mediate chromosomal inversions (Caceres et al., 1999). An intriguing hypothesis is that the inversion event in our Ambras patient is also transposase-mediated.

Observation of the small insertions and deletions at the breakpoint junctions, is consistent with similar observations for other translocations (Zhang et al., 2002; Reiter et al., 2003; Abeysinghe et al., 2003). The lack of sequence similarity between the sequences surrounding the 8p and 8q breakpoints suggests that the inversion did not occur by a homologous recombination event. The lack of a recombination "hotspot" at the breakpoint junctions might explain why this particular pericentric inversion of chromosome 8 is so rare. We are unaware of any other cases in the literature that are reported to have this same rearrangement.

Since the inversion breakpoints in our patient do not disrupt the coding sequence of a gene, we believe that a position effect might be the cause of the mutant phenotype in this Ambras syndrome patient. A position effect is a phenomenon reflecting alterations in gene expression that result from changes in the gene's position relative to its normal chromosomal context rather than intragenic deletions or mutations (Kleinjan and van Heyningen, 1998). Position effects have been implicated as causative events in a number of human disorders such as campomelic dysplasia (Wirth et al., 1996), aniridia (Fantes et al., 1995), X-linked deafness type 3 (DFN3) (de Kok et al., 1995), and Saethre-Chotzen syndrome (Krebs et al., 1997). Moreover, it has been shown that the changes in gene expression can result even when the breakpoints are up to one megabase away from the gene, and irrespective of whether they occur 5′ or 3′ of the gene of interest (Kleinjan and van Heyningen, 1998).

In summary, we have cloned the breakpoints in a novel inversion of chromosome 8 inv (8)(p11.2q23.1) in a patient with Ambras syndrome. We have assembled a contig across the inversion breakpoint interval, and identified all transcripts in the vicinity of the breakpoint. We determined that the breakpoint does not result in the disruption of the coding sequence of a gene, but rather occurs within repetitive DNA elements. Search for putative regulatory elements in the genomic sequence surrounding the breakpoint, and analysis of genes that map further away from the breakpoint is likely to provide a better understanding of the molecular mechanisms that are involved in the etiology of Ambras syndrome.

Acknowledgements

The authors would like to thank patient ME-1 and her family for participating in this study. We are grateful to Dr. Riccardo Dalla Favera and Thomas Boulin for invaluable technical advice on breakpoint subcloning strategies. We appreciate the insightful conversations with Drs. Timothy Bestor and Gary Swergold. We would also like to thank Antonio Sobrino, Taknida Tubo and C-Y Yu for their technical assistance.

References

Abeysinghe SS, Chuzhanova N, Krawczak M, Ball EV, Cooper DN: Translocation and gross deletion breakpoints in human inherited disease and cancer I: nucleotide composition and recombination-associated motifs. Hum Mutat 22:229–244 (2003).

Adams JC, Tucker RP: The thrombospondin type I repeat (TSR) superfamily: diverse proteins with related roles in neuronal development. Dev Dyn 218:280–299 (2000).

Balducci R, Toscano V, Tedeschi B, Mangiantini A, Toscano R, Galasso C, Cianfarani S, Boscherini B: A new case of Ambras syndrome associated with a paracentric inversion (8) (q12; q22). Clin Genet 53:466–468 (1998).

Baumeister FA, Egger J, Schildhauer MT, Stengel-Rutkowski S: Ambras Syndrome: delineation of a unique hypertrichosis universalis congenita and association with a balanced pericentric inversion (8) (p11.2q22). Clin Genet 44:121–128 (1993).

Belloni E, Muenke M, Roessler E, Traverso G, Siegel-Bartelt J, Frumkin A, Mitchell HF, Donis-Keller H, Helms C, Hing AV, Heng HHQ, Koop B, Martindale D, Rommens JM, Tsui L-C, Scherer SW: Identification of Sonic Hedgehog as a candidate gene responsible for holoprosencephaly. Nature Genet 14:353–356 (1996).

Caceres M, Ranz JM, Barbadilla A, Long M, Ruiz A: Generation of a widespread *Drosophila* inversion by a transposable event. Science 285:415–418 (1999).

Crackower MA, Scherer SW, Rommens JM, Hui CC, Poorkaj P, Soder S, Cobben JM, Hudgins L, Evans JP, Tsui LC: Characterization of the split hand/split foot malformation locus SHFM1 at 7q21.3→q22.1 and analysis of a candidate gene for its expression during limb development. Hum Mol Genet 5:571–579 (1996).

De Kok YJM, Merkx GFM, van der Maarei SM, Huber I, Malcolm S, Ropers H-H, Cremers FPM: A duplication/paracentric inversion associated with familial X-linked deafness (DFN3) suggests the presence of a regulatory element more than 400 kb upstream of the *POU3F4* gene. Hum Mol Genet 4:2145–2150 (1995).

Fantes J, Redeker B, Breen M, Boyle S, Brown J, Fletcher J, Jones S, Bickmore W, Fukushima Y, Mannens M, Danes S, van Heyningen V, Hanson I: Aniridia-associated cytogenetic rearrangements suggest that a position effect may cause the mutant phenotype. Hum Mol Genet 4:415–422 (1995).

Gessler M, Simola KO, Bruns GA: Cloning of breakpoints of a chromosome translocation identifies the AN2 locus. Science 244:1575–1578 (1989).

Hoffman CS, Winston F: A 10-minute DNA preparation from yeast efficiently releases autonomous plasmids for transformation of *Escherichia coli*. Gene 57:267–272 (1987).

Kleinjan DJ, van Heyningen V: Position effect in human genetic disease. Hum Mol Genet 7:1611–1618 (1998).

Kolomietz E, Meyn MS, Pandita A, Suire JA: The role of Alu repeat clusters as mediators of recurrent chromosomal aberrations in tumors. Genes Chrom Cancer 35:97–112 (2002).

Krebs I, Weis I, Hudler M, Rommens JM, Roth H, Scherer SW, Tsui L-C, Fuchtbauer E-M, Grzeschik K-H, Tsuji K, Kunz J: Translocation breakpoint maps 5 kb 3′ from *TWIST* in a patient affected with Saethre-Chotzen syndrome. Hum Mol Genet 6:1079–1086 (1997).

Marchetti A, Buttitta F, Miyazaki S, Gallahan D, Smith G, Callahan R: Int-6, a highly conserved, widely expressed gene, is mutated by mouse mammary tumor virus in mammary preneoplasia. J Virol 69:1932–1938 (1995).

Nowakowski TK, Scholz A: Das Schicksal behaarter Menschen im Wandel der Geschichte. Hautarzt 28:593–599 (1977).

Online-MIM, 2000: http://www3.ncbi.nlm.nih.gov/Omim/searchomim.html.

Rasmussen SB, Kordon E, Callahan R, Smith GH: Evidence for the transforming activity of a truncated Int6 gene in vitro. Oncogene 20:5291–5301 (2001).

Reiter A, Saussele S, Grimwade D, Wiemels JL, Segal MR, Lafage-Pochitaloff M, Waltz C, Weisser A, Hochhaus A, Willer A, Reichert A, Buchner T, Lengfelder E, Hehlmann R, Cross NCP: Genomic anatomy of the specific reciprocal translocation t(15;17) in acute promyelocytic leukemia. Genes Chromosomes Cancer 36:175–188 (2003).

Reiter LT, Murakami T, Koeuth T, Penrao L, Muzny DM, Gibbs RA, Lupski JR: A recombination hotspot responsible for two inherited peripheral neuropathies is located near a *mariner* transposon-like element. Nat Genet 12:288–297 (1996).

Robertson HM: Members of pogo superfamily of DNA-mediated transposons in the human genome. Mol Gen Genet 252:761–766 (1996).

Smith AF, Riggs AD: Tiggers and DNA transposon fossils in the human genome. Proc Natl Acad Sci USA 93:1443–1448 (1996).

Speck SH, Strominger JL: Epstein-Barr virus transformation. Prog Nucleic Acid Res Mol Biol 34:189–207 (1987).

Srivastava AK, Montonen O, Saarialho-Kere U, Chen E, Baybayan P, Pispa J, Limon J, Schlessinger D, Kere J: Fine mapping of the EDA gene: a translocation breakpoint is associated with a CpG island that is transcribed. Am J Hum Genet 58:126–132 (1996).

Tadin M, Braverman E, Cianfarani S, Sobrino AJ, Levy B, Christiano AM, Warburton D: Complex cytogenetic rearrangement of chromosome 8q in a case of Ambras syndrome. Am J Med Genet 102:100–104 (2001).

Torbus O, Sliwa F: Ambras syndrome—a form of generalized congenital hypertrichosis. Pol Merkuriusz Lek 69:238–240 (2002).

Wagner A, van der Klift H, Franken P, Wijnen J, Breukel C, Berrookove V, Smits R, Kinarsky Y, Barrows A, Franklin B, Lynch J, Lynch H, Fodde R: A 10-Mb paracentric inversion of chromosome arm 2p inactivates MSH2 and is responsible for hereditary nonpolyposis colorectal cancer in a North American kindred. Genes Chromosomes Cancer 35:49–57 (2002).

Wirth J, Wagner T, Meyer J, Pfeiffer RA, Tietze H-U, Schempp W, Scherer G: Translocation breakpoints in three patients with campomelic dysplasia and autosomal sex reversal map more than 130 kb from SOX9. Hum Genet 97:186–193 (1996).

Yano K, Brown LF, Lawel J, Miyakawa T, Detmar M: Thrombospondin-1 plays a critical role in the induction of hair follicle involution and vascular regression during the catagen phase. J Invest Dermatol 120:14–19 (2003).

Yen HC, Gordon C, Chang EC: *Schizosaccharomyces pombe* Int6 and Ras homologs regulate cell division and mitotic fidelity via the proteasome. Cell 112: 207–217 (2003).

Zhang Y, Strissel P, Strick R, Chen J, Nucifora G, Le Beau MM, Larson RA, Rowley JD: Genomic DNA breakpoints in AML/RUNX1 and ETO cluster with topoisomerase II cleavage and Dnase I hypersensitive sites in t(8;21) leukemia. Proc Natl Acad Sci USA 99:3070–3075 (2002).